HOKKAIDO UNIVERSITY

Title	Vapour and mechanically induced chromic behaviour of platinum complexes with a dimer-of-dimer motif and the effects of heterometal ions
Author(s)	Ohba, Tadashi; Kobayashi, Atsushi; Chang, Ho-Chol; Kato, Masako
Citation	Dalton Transactions, 42(15), 5514-5523 https://doi.org/10.1039/c3dt33100h
Issue Date	2013-02
Doc URL	http://hdl.handle.net/2115/54595
Type	article (author version)
File Information	OhbaMPt13MK.pdf

Instructions for use

ARTICLE TYPE

Vapour and mechanically induced chromic behaviour of platinum complexes with a dimer-of-dimer motif and the effects of hetero metal ions

Tadashi Ohba, Atsushi Kobayashi, Ho-Chol Chang, Masako Kato*

Heterodinuclear complexes, *syn*-[MPt(μ-pyt)$_2$(bpy)$_2$]$^{n+}$ (*syn*-[**MPt**], M = Pd^{2+}, Au^{3+}, Hpyt = pyridine-2-thiol, bpy = 2,2′-bipyridine) were synthesized as a selective geometrical isomer by stepwise complexation. X-ray analyses of the hexafluorophosphate salts of these complexes proved their dinuclear structures with
10 short M···Pt distances (2.9084(4) Å for *syn*-[**PdPt**] and 2.9071(4) Å for *syn*-[**AuPt**]), similar to the homodinuclear complex (2.9292(2) Å for *syn*-[**PtPt**]). In the *syn*-[**PdPt**] crystal, two dinuclear motifs are arranged closely in a head-to-head manner with a short Pt···Pt distance (3.3757(3) Å), forming a dimer-of-dimer structure as in the case of *syn*-[**PtPt**], whereas the corresponding crystal of *syn*-[**AuPt**] has a discrete arrangement of the dinuclear motifs. By the isomerisation of *syn*-[**PdPt**], *anti*-[**PdPt**] with
15 equivalent environments of the Pd^{2+} and Pt^{2+} ions was also obtained successfully. *Syn*-[**PdPt**](PF$_6$)$_2$ exhibits vapochromic behaviour based on the absorption/desorption of CH$_3$CN vapour, similar to that observed for *syn*-[**PtPt**](PF$_6$)$_2$. The reversible structural transformations induced by the uptake and release of CH$_3$CN molecules were investigated by powder and single-crystal X-ray diffraction studies. These revealed that the vapochromic behaviour was based on the interconversion between two phases, the
20 dimer-of-dimer structure with a short Pt···Pt distance and a π-π stacked arrangement with no Pt···Pt intermolecular interaction. The introduction of the hetero metal ions enabled control of the colour region: orange ↔ red for *syn*-[**PdPt**] vs. light red ↔ dark red for *syn*-[**PtPt**], reflecting the weaker metal-metal interaction between Pd^{2+} and Pt^{2+} ions in the dinuclear motif. In addition, these complexes were found to exhibit mechanochromic behaviour based on a crystal-to-amorphous transformation upon grinding, and
25 the reconstruction of the crystal structures by vapour sorption.

Introduction

There has been considerable interest in recent years in the development of vapochromic sensor materials for the detection of volatile organic compounds (VOCs).[1] In particular, assembled
30 platinum(II) complexes with d^8 configurations provide rich chromotropic chemistry on the basis of changes in intermolecular interactions such as π-π, donor-acceptor, and metal-metal interactions induced by the absorption/desorption of vapour molecules.[2] Thus, they are promising materials for naked-eye
35 perceivable chemosensors for small molecules. However, vapochromic systems with clearly elucidated mechanisms are still limited despite the increasing numbers of reported systems, and detailed investigation is necessary to achieve their rational design.

We previously reported a homometallic dinuclear
40 platinum(II) complex, [Pt$_2$(μ-pyt)$_2$(bpy)$_2$]$^{2+}$ (pyt = pyridine-2-thiolate, bpy = 2,2′-bipyridine),[3] which has two geometrical isomers, the *syn*- and *anti*-isomers (*syn*-[**PtPt**] and *anti*-[**PtPt**]), corresponding to the case of M = Pt^{2+} in Scheme 1. The hexafluorophosphate salt of *syn*-[**PtPt**] exhibits an interesting
45 vapour-induced colour change between dark-red and light-red on the absorption/desorption of acetonitrile (CH$_3$CN) molecules.
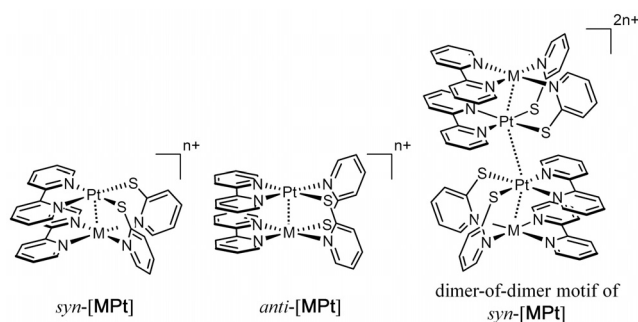
Scheme 1 Homo- (M = Pt^{2+}) and heterodinuclear motifs.

Concomitantly, a remarkable luminescence switching occurs for
50 the dinuclear complex. The dark-red form (CH$_3$CN-included form) of the *syn*-isomer crystal adopts a dimer-of-dimer structure, wherein the four Pt ions of two *syn*-[**PtPt**] cations are arranged so as to generate an intermolecular metal–metal interaction (Scheme 1). Similar dimer-of-dimer structures are known for mixed-
55 valence platinum complexes (*i.e.* platinum blues).[4] Though there is no chemical bond between intermolecular divalent platinum ions for *syn*-[**PtPt**], the expansion of the electronic metal-metal

interactions from the dimer to the dimer-of-dimer structure could lower the energy of the metal-metal-to-ligand charge transfer (MMLCT) transition.[3] Thus, we proposed that the vapochromic behaviour for this system would occur by the change of the Pt···Pt electronic interactions between the dinuclear complexes. To explore the electronic effects of the metal-metal interactions on the vapochromic behaviour, it would be effective to introduce different metal ions into the same dinuclear motif. Fortunately, the structural features of *syn*-[**PtPt**] strongly suggest that the molecular framework would be a good candidate for the incorporation of two different metal ions because the bridging ligand (pyt) provides two different coordination environments.

In this work, we newly synthesized two heterodinuclear metal complexes using d[8] metal ions, *syn*-[MPt(μ-pyt)$_2$(bpy)$_2$]$^{n+}$ (*syn*-[**MPt**]; M = Pd^{2+} (n = 2), M = Au^{3+} (n = 3)), as well as *anti*-[PdPt(μ-pyt)$_2$(bpy)$_2$]$^{2+}$ (*anti*-[**PdPt**]). The hexafluorophosphate salt of *syn*-[**PdPt**] exhibited vapochromic behaviour with different colour changes from that of *syn*-[**PtPt**], while *syn*-[**AuPt**] and *anti*-[**PdPt**] did not show any vapochromic behaviour. We also succeeded in the direct observation of the structural transformation induced by the absorption/desorption of vapour molecules for *syn*-[**PtPt**] and *syn*-[**PdPt**] on the basis of X-ray diffraction studies. Herein, the particular mechanism of the vapochromism and the effects of hetero metal ions based on the metal-metal interactions for these dinuclear systems are discussed, considering other findings by UV-vis spectroscopy and thermal analysis.

Experimental

Materials and synthesis. All starting materials were used as received from commercial sources, and the solvents were used without purification. 2,2′-Bipyridine (bpy), pyridine-2-thiol (Hpyt) and PdCl$_2$ were purchased from Wako. K$_2$PtCl$_4$ and HAuCl$_4$ were purchased from Tanaka Holdings. [PtCl$_2$(bpy)],[5] [PdCl$_2$(bpy)],[6] [AuCl$_2$(bpy)](NO$_3$),[7] [Pt(pyt)$_2$(bpy)],[8] and *syn*-[Pt$_2$(μ-pyt)$_2$(bpy)$_2$](PF$_6$)$_2$[3] were prepared according to methods previously reported.

Syn-[PdPt(μ-pyt)$_2$(bpy)$_2$](PF$_6$)$_2$ (*syn*-[**PdPt**](PF$_6$)$_2$). To a suspension of [PdCl$_2$(bpy)] (33.3 mg, 0.1 mmol) in H$_2$O (6 mL) was added silver nitrate (34.0 mg, 0.2 mmol) in H$_2$O (4 mL). The reaction mixture was stirred for 2 h in the dark at 60°C, and then filtered to remove silver chloride. The pale yellow filtrate was treated with [Pt(pyt)$_2$(bpy)] (57.1 mg, 0.1 mmol) in H$_2$O (2 mL). The resulting red solution was allowed to stir for 30 min and NH$_4$PF$_6$ (81.5 mg, 0.5 mmol) in H$_2$O (2 mL) was added. An orange precipitate was immediately deposited, which was then filtered and dried under reduced pressure. Yield: 103.5 mg (92.1%). Red polyhedral crystals (*syn*-isomer) suitable for X-ray diffraction were obtained as an CH$_3$CN-solvated form by the diffusion method using Et$_2$O/ CH$_3$CN at 4°C. ^{1}H NMR (DMSO-d_6): δ 7.30 (t, 2H), 7.39 (td, 2H), 7.44 (d, 2H), 7.59 (t, 2H), 7.69 (t, 2H), 7.82 (d, 2H), 8.15 (d, 2H), 8.18 (td, 2H), 8.27 (t, 2H), 8.35 (d, 2H), 8.87 (d, 2H), 9.07 (d, 2H). Anal. Calcd. for C$_{30}$H$_{24}$F$_{12}$N$_6$P$_2$PdPtS$_2$: C, 32.05; H, 2.15; N, 7.48; S, 5.71. Found: C, 32.00; H, 2.26; N, 7.46; S, 5.87.

Anti-[PdPt(μ-pyt)$_2$(bpy)$_2$](PF$_6$)$_2$ (*anti*-[**PdPt**](PF$_6$)$_2$). The powder of the *syn*-[**PdPt**] complex (98.3 mg, 87 μmol) was dissolved in CH$_3$CN (1 mL) and allowed to stand for 1 day at room temperature (RT). After 1 day, a crystal suitable for X-ray diffraction was obtained as an CH$_3$CN-solvated form by the

Table 1 Crystallographic data of hexafluorophosphate salts of [**MPt**]

	syn-[**PdPt**](PF$_6$)$_2$·1.5CH$_3$CN	*anti*-[**PdPt**](PF$_6$)$_2$·CH$_3$CN	*syn*-[**AuPt**](PF$_6$)$_3$·2CH$_3$CN
Formula	C$_{33}$H$_{28.5}$N$_{7.5}$F$_{12}$P$_2$PdPtS$_2$	C$_{32}$H$_{27}$N$_7$F$_{12}$P$_2$PdPtS$_2$	C$_{34}$H$_{30}$N$_8$AuF$_{18}$P$_3$PtS$_2$
Formula weight	1185.68	1165.15	1441.73
Crystal system	Orthorhombic	Monoclinic	Monoclinic
Space group	*Pbcn* (#60)	*P*2$_1$/*c* (#14)	*C*2/*c* (#15)
a (Å)	27.586(4)	24.774(2)	22.673(3)
b (Å)	13.543(2)	11.1858(8)	13.050(2)
c (Å)	21.015(3)	14.211(1)	30.037(5)
α (°)	90	90	90
β (°)	90	92.3480(8)	100.1920(5)
γ (°)	90	90	90
V (Å^3)	7851(2)	3934.7(5)	8747(2)
Z	8	4	8
T (K)	150	150	150
D_{calcd} (g cm^{-3})	2.006	1.967	2.189
μ (Mo Kα) (cm^{-1})	42.87	42.74	68.66
R_1[a] ($F^2 > 2\sigma(F^2)$)	0.0605	0.0477	0.0504
wR_2[b] (all data)	0.1087	0.1186	0.1169

[a] $R_1 = \Sigma ||F_o| - |F_c||/\Sigma |F_o|$. [b] $wR_2 = [\Sigma w(F_o^2 - F_c^2)/\Sigma w(F_o^2)^2]^{1/2}$, $w = [\sigma_c^2(F_o^2) + (xP)^2 + yP]^{-1}$, $P = (F_o^2 - 2F_c^2)/3$.

diffusion method using Et_2O/CH_3CN at RT. Yield: 45.2 mg (46.0%). ^{1}H NMR (DMSO-d_6): δ 7.21–7.35 (m, 4H), 7.55 (d, 1H), 7.46 (t, 4H), 7.77 (t, 1H), 7.90 (t, 1H), 8.38 (d, 2H), 8.74 (d, 2H), 8.83 (d, 2H). Anal. Calcd. for $C_{30}H_{24}F_{12}N_6P_2PdPtS_2$: C, 32.05; H, 2.15; N, 7.48. Found: C, 31.83; H, 2.30; N, 7.47.

Syn-[AuPt(μ-pyt)$_2$(bpy)$_2$](PF$_6$)$_3$ (*syn*-[**AuPt**](PF$_6$)$_3$). [AuCl$_2$(bpy)](NO$_3$) (72.7 mg, 0.15 mmol) was suspended in H_2O (10 mL) and silver nitrate (50.4 mg, 0.3 mmol) in H_2O (5 mL) was added. The reaction mixture was stirred for 3 days in the dark at RT and then filtered to remove silver chloride. The pale yellow filtrate was treated with [Pt(pyt)$_2$(bpy)] (57.1 mg, 0.1 mmol) in H_2O (2.5 mL). The resulting solution was stirred for 30 min at room temperature. NH$_4$PF$_6$ (81.5 mg, 0.5 mmol) in H_2O (2 mL) was added and the resulting red precipitate was filtered. The red filtrate was allowed to stand for ca. 10 days and a red crystalline solid was obtained (yield: 22.6 mg (17%)). Dark red crystals suitable for X-ray diffraction were obtained as an CH_3CN-solvated form via the diffusion of EtOH into a CH_3CN solution of the crude material. ^{1}H NMR (DMSO-d_6) for [AuPt(pyt)$_2$(bpy)$_2$](PF$_6$)$_3$: δ 7.45 (m, 2H), 7.70 (t, 2H), 7.84 (d, 2H), 7.86 (d, 2H), 8.11 (t, 2H), 8.24 (d, 2H), 8.33 (d, 4H), 8.53 (t, 2H), 8.64 (d, 2H), 9.02 (d, 2H), 9.10 (d, 2H). Anal. Calcd. for $C_{30}H_{24}AuF_{18}N_6P_3PtS_2$: C, 26.50; H, 1.78; N, 6.18; S, 4.72. Found: C, 26.38; H. 1.90; N, 5.92; S, 4.67.

Physical measurements

^{1}H NMR spectra were recorded on a JEOL JNM-EX270 FT-NMR system. Elemental analyses were performed by a Micro Corder JM 10 analyser at the Analysis Centre, Hokkaido University. UV–vis spectra in solution were recorded on a Shimadzu MultiSpec-1500 spectrophotometer. UV–vis diffuse reflectance spectra were obtained on a Hitachi U-3000 spectrometer equipped with an integrating sphere apparatus. Thermogravimetry and differential thermal analysis were performed using a Rigaku ThermoEvo TG8120 analyzer.

X-ray diffraction measurements and structure analyses

A summary of the crystallographic data of the single-crystal X-ray diffraction for the *syn*-[**PdPt**], *anti*-[**PdPt**], and *syn*-[**AuPt**] complexes is given in Table 1. Each crystal was mounted on a glass fibre with silicon grease. All measurements for the three crystals were made on a Rigaku AFC-7R diffractometer with Mercury CCD area detector, graphite monochromated Mo-$K\alpha$ radiation (λ = 0.71069 Å) and a rotating anode generator. The data were corrected for Lorentz and polarization effects. Diffraction data were collected and processed using CrystalClear.[9] The structures were solved using direct methods (SIR92)[10] and expanded using Fourier techniques (DIRDIF99).[11] Full-matrix least-squares structural refinement based on F^2 was employed. The non-hydrogen atoms were refined anisotropically. The hydrogen atoms were refined using a riding model. For *anti*-[**PdPt**], the Pt and Pd atoms were found to be completely disordered. They were placed on same site at each of the two metal centres with a half occupancy, and their positions were refined. All calculations were performed using CrystalStructure,[12] a crystallographic software package except for refinement, which was performed using SHELXL97.[13] Full crystallographic data have been deposited with the Cambridge Crystallographic Data Centre (CCDC 917078–917080).

Single-crystal to single-crystal transformation for *syn*-[**PtPt**] was performed on a Rigaku AFC-8 diffractometer equipped with the nitrogen gas flow variable temperature controller. The data reduction and structure analysis were carried out in a similar manner described above. The crystallographic details are summarized in the supplementary information.

Powder X-ray diffraction measurements were carried out with Cu $K\alpha$ radiation using a Rigaku SmartLab diffractometer.

Results and discussion

Regioselective synthesis of heterodinuclear complexes. We previously reported the one-step synthesis of homodinuclear platinum complexes *syn*- and *anti*-[**PtPt**] by the reaction of [PtCl$_2$(bpy)] and Hpyt.[3] The *syn* and *anti* geometrical isomers were produced as a mixture and the isolation of the *syn* isomer of the minor component was troublesome in this method. For the regioselective synthesis of the *syn* isomer, a stepwise complexation as shown in Scheme 2 should be favourable, in particular, it should be a good way to prepare heterodinuclear complexes. Recently, Lippert et al. reported that the stepwise synthesis of a *syn* isomer of heterodinuclear complex of Pd(en) (en = ethylenediamine) and Pt(bpy) units by using two cytosinato bridges. However, they could not obtained the corresponding heterodinuclear complex from Pd(bpy) and Pt(bpy) units but a Pd-Pt-Pd trinuclear motif with an *anti*-configration.[14] We succeeded in the formation of the *syn* isomer of heterodinucler complex comprising Pd(bpy) and Pt(bpy) units by using the pyt bridging ligand. The different affinities of the coordinating atoms (N and S) in the pyt ligand to Pd^{2+} and Pt^{2+} ions would be more advantageous for the regioselective synthesis. In the first step, the mononuclear complex [Pt(pyt)$_2$(bpy)] including S-coordinated pyt ligands was selectively prepared. In the second step, the Pd^{2+} ion was introduced by the coordination of nitrogen atoms of the pyt ligands. Applying this stepwise synthesis, the *syn*-[**AuPt**] complex was also obtained.

In solution at room temperature, the isomerisation from *syn*- to *anti*-isomer is very slow for [**PtPt**]. In the case of the palladium–platinum mixed complex, [**PdPt**], however, the isomerization was faster than that for the dinuclear platinum complex, and *syn*-[**PdPt**] was almost completely converted to *anti*-[**PdPt**] within a day at RT (Fig. S1). The crystal of *anti*-[**PdPt**] was thus isolated from the solution. On the other hand, isomerization of *syn*-[**AuPt**] was not observed, but a precipitate due to decomposition was deposited after one day in CH_3CN.
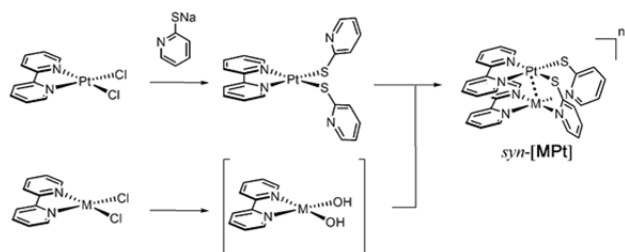
Scheme 2 Regioselective synthesis of *syn*-[**MPt**] motif.
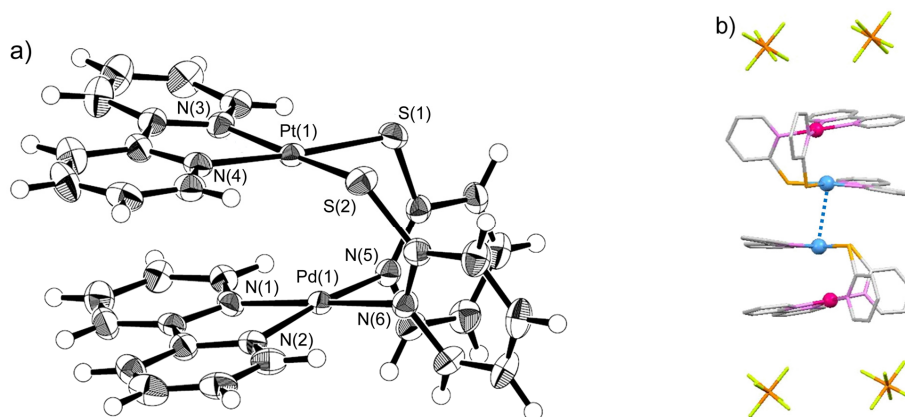
Fig. 1 a) Molecular structure of *syn*-**[PdPt]** (50% probability ellipsoids). b) The dimer-of-dimer structure of *syn*-**[PdPt]**. The PF_6^- ions located at the top and bottom of the dimer-of-dimer motif are also included. The intermolecular Pt⋯Pt contact is shown by the dotted line.
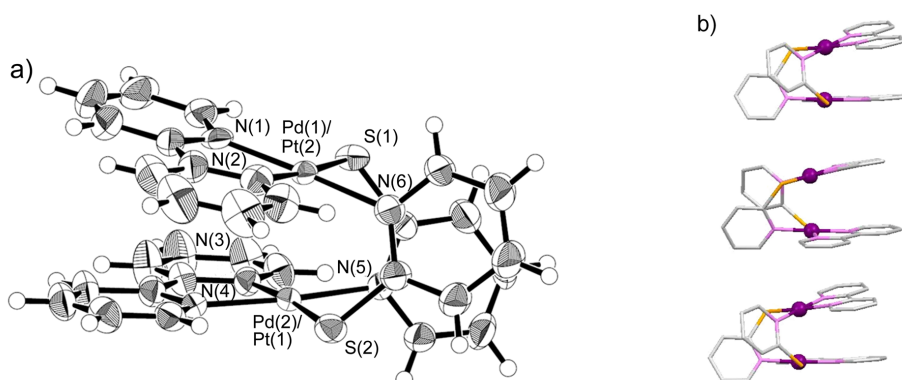

Fig. 2 a) Molecular structure of *anti*-**[PdPt]** (50% probability ellipsoids). The Pt and Pd atoms are disordered with half occupancies. b) The loose stacked structure of *anti*-**[PdPt]**.
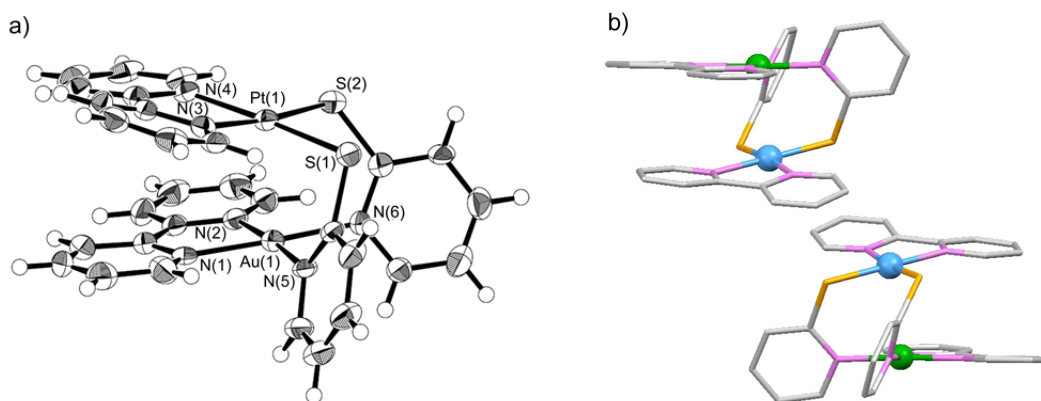

Fig. 3 a) Molecular structure of *syn*-**[AuPt]** (50% probability ellipsoids). b) No interactive arrangement of two adjacent complexes for *syn*-**[AuPt]**.

Crystal structures. Figs. 1, 2, and 3 show the structures of *syn*-[**PdPt**], *anti*-[**PdPt**], and *syn*-[**AuPt**] in the CH$_3$CN-included forms of the hexafluorophosphates, respectively. The selected interatomic distances and dihedral angles are shown in Table 2 as well as those of *syn*-[**PtPt**]. The hexafluorophosphate salt of *syn*-[**PdPt**] was found to be isostructural with that of *syn*-[**PtPt**].[3] As shown in Fig. 1a, the Pd^{2+} ion in *syn*-[**PdPt**] was surrounded by four nitrogen atoms while the Pt^{2+} ion was coordinated by two nitrogen atoms and two sulphur atoms. Reasonable values for the thermal factors for Pt and Pd supported the assignment in this structure, indicating no disorder between the two metal ions.

Observed Pd-N, Pt-S, and Pt-N bond distances are typical values. The dihedral angle between the Pd-bpy and Pt-bpy planes (the least-square planes defined by the metal ion and non-hydrogen atoms of the bpy ligand) is about 14° which is similar to that of *syn*-[**PtPt**]. The intramolecular Pd⋯Pt distance (2.9084(4) Å) is also comparable to that of the *syn*-[**PtPt**] complex (2.9168(3) Å), and shorter than the sum of the van der Waals radii of Pt and Pd (3.38 Å), suggesting that a metal–metal interaction is in effect in the heterodinuclear complex. Interestingly, two *syn*-[**PdPt**] units were arranged so that the Pt ions are closely located, as shown in Fig. 1b. This dimer-of-dimer structure is nearly the same as that

	syn-[**PtPt**](PF$_6$)$_2$ [a]	*syn*-[**PdPt**](PF$_6$)$_2$	*syn*-[**AuPt**](PF$_6$)$_3$	*anti*-[**PdPt**](PF$_6$)$_2$
Selected distance(Å)	M = Pt	M = Pd	M = Au	M = Pd
Pt–S	2.281(2), 2.291(2)	2.293(2), 2.282(2)	2.299(2), 2.318(2)	2.297(2), 2.309(2)
Pt–N(bpy)	2.062(7), 2.076(6)	2.070(5), 2.060(5)	2.099(5), 2.097(5)	2.018(6), 2.045(6)
M–N(bpy)	2.010(6), 2.033(6)	2.023(5), 2.012(5)	2.016(5), 2.024(5)	2.058(6), 2.026(5)
M–N(pyt)	2.027(5), 2.040(6)	2.040(5), 2.034(5)	2.029(5), 2.030(5)	2.023(5), 2.032(5)
M···Pt (intramolecular)	2.9168(3)	2.9084(4)	2.9292(3)	2.9767(5)
Pt···Pt (intermolecular)	3.384(1)	3.3757(3)	5.1899(3)	4.2893(3)
Dihedral angles(°)				
bpy(M)/bpy(Pt)	14.22(8)	14.54(6)	13.93(7)	13.3(1)
bpy(Pt)/pyt	71.7(2), 88.3(1)	71.9(1), 88.1(1)	72.9(1), 81.0(1)	65.5(1), 71.1(1)
bpy(M)/pyt	79.4(1), 98.3(1)	79.9(1), 98.06 (8)	67.1(1) ,70.8(1)	74.3(1), 72.1(1)

[a] ref. 3.

of *syn*-[**PtPt**]. The intermolecular distance between the two Pt ions for *syn*-[**PdPt**] (3.3757(3) Å) is shorter than twice the van der Waals radius of Pt (3.50 Å), as in the case of *syn*-[**PtPt**] (3.384(1) Å),[3] strongly suggesting a metal-metal interaction between two *syn*-[**PdPt**]. Interestingly, a dimer-of-dimer structure for [PtPd(bpy)$_2$(DMGI)$_2$] (DMGI = 3,3-dimethylglutarimidate) adopted an arrangement which faced two Pd^{2+} coordination sites instead of the Pt^{2+} sites, and the Pd···Pd distance was very long (3.829(2) Å), suggesting no intermolecular metal-metal interaction.[15]

Figure 2 depicts the structure of *anti*-[**PdPt**]. Each metal ion is surrounded by three nitrogen atoms and one sulphur atom. In contrast with *syn*-[**PdPt**], the Pt and Pd ions for *anti*-[**PdPt**] were found to be completely disordered at the two metal sites. The heterodinuclear structure was confirmed by the FAB-MS spectrum of the crystalline sample which gave only the peaks originating from the heterodinuclear complex [**PdPt**] (*m/z* = 977.1 for {[**PdPt**]·PF$_6$}$^+$, Fig. S2). The intramolecular Pd···Pt distance for *anti*-[**PdPt**] was 2.9765(3) Å, which also suggests the existence of a metal-metal interaction, although it is slightly longer than that of *syn*-[**PdPt**]. Considering that the torsion angle between the bpy ligands about the Pd-Pt axis (N1–M···M'–N3 = 40.3° av.) is much larger for *anti*-[**PdPt**] than for *syn*-[**PdPt**] (N1-Pd···Pt–N3 = 17.8° av.), as well as the smaller dihedral angles between the bpy and pyt ligands for *anti*-[**PdPt**] than for *syn*-[**PdPt**] (Table 2), the longer Pd···Pt distance of *anti*-[**PdPt**] is attributable to the larger deformation of the dinuclear framework compared with that of *syn*-[**PdPt**]. In the crystal, *anti*-[**PdPt**] forms a columnar structure with intermolecular π-π stacking (3.35 Å) between the bpy ligands (Fig. 2b), in which the stack is a rather shifted arrangement to avoid the steric hindrance of the pyt ligand. The deformation of the dinuclear framework in *anti*-[**PdPt**] could be due to adjustment of the packing structure. As a result, the intermolecular metal-metal distance (4.3 Å) in the column is too long for a metal-metal interaction.

Figure 3a shows the molecular structure of *syn*-[**AuPt**]. As in the case of *syn*-[**PdPt**], the introduced Au^{3+} ion occupies the N$_4$ coordination site while the Pt ion is coordinated by two sulphur and two nitrogen atoms. The intramolecular Au···Pt distance (2.9292(3) Å) is comparable to the Pt···Pt distance of the *syn*-

[**PtPt**] complex and shorter than the sum of the van der Waals radii (3.41 Å), suggesting that a metal-metal interaction is in effect in the Pt(II)-Au(III) dinuclear complex. Although the stacking structure of Pt^{2+} and monovalent Au$^+$ ions is well known,[16] assembled systems of Au(III) complexes have not often been reported. The dimeric structure of [Au(C^N^N-dpp)Cl]$^+$ (C^N^N-dppH = 2,9-diphenyl-1,10-phenanthroline) was reported to provide a long Au···Au distance (3.6 Å).[17] A π-π stacking structure was found for a Au(III) complex, [Au(C^N^C)(C≡CPh)] (HC^N^CH = 2,6-diphenylpyridine), where Au···Au was 5.003(1) Å.[18] Bosnich et al. reported that the interaction between Pt^{2+} and Au^{3+} was unfavourable on the basis of experiments carried out for the adduct formation of a Pt(II) dinuclear complex with a terpyridine derivative, and a Au(III) complex, [Au(C^N^C)CN].[19] To the best of our knowledge, *syn*-[**AuPt**] is the first example that includes Au^{3+} and Pt^{2+} ions in close arrangement. The key point for *syn*-[**AuPt**] is that no intermolecular interactions could be observed between adjacent dinuclear complexes (Pt···Pt = 5.1899(3) Å) in contrast to the cases for *syn*-[**PdPt**] and *syn*-[**PtPt**] (Fig. 3b). This is due to the higher positive charge (3+) of *syn*-[**AuPt**]. There are three PF$_6^-$ anions per one [**AuPt**] cation in the crystal, which prevents the complexes from forming the dimer-of-dimer structure with a short intermolecular Pt···Pt contact.

Vapochromic behaviour. The *syn*-[**PdPt**] salt exhibits vapochromic behaviour, similarly to the isomorphous *syn*-[**PtPt**] salt. Characteristically, *syn*-[**PdPt**] exhibited a quite different colour change compared with the *syn*-[**PtPt**] salt (Fig. 4). For *syn*-[**PdPt**], the CH$_3$CN-included form is red in colour and air-stable at room temperature (Fig. 4A). However, a colour change from red to orange was observed upon moderate heating (50°C) under dry Ar atmosphere or vacuum (Fig. 4B). Upon exposure to CH$_3$CN vapour, the orange colour reverted to the original red colour in a few minutes. Such colour changes occurred reversibly by the absorption and desorption of CH$_3$CN vapour as proven by an adsorption isotherm and thermogravimetric analyses for *syn*-[**PdPt**] (Figs. S3 and S4). The absence of CH$_3$CN molecules in the orange form was also confirmed by ^{1}H NMR measurements (Fig. S5). For comparison of the vapour response of the *syn*-

Fig. 4 Photographs of powder samples: A and D) vapour-included forms; B and E) desorbed forms; and C and F) ground forms, for *syn*-[**PdPt**] and *syn*-[**PtPt**], respectively.

[**MPt**] complexes, UV-vis diffuse reflectance spectra of the solid samples are shown in Fig. 5. For both *syn*-[**PdPt**] and *syn*-[**PtPt**] salts, distinct spectral changes were confirmed on exposure of the samples after heat treatment to CH_3CN vapour (Figs. 5a and 5b). In contrast, the *syn*-[**AuPt**] salt exhibits no chromic behaviour and the solid state spectrum is essentially the same as that in solution (Fig. 5c). The blue-shifted spectra of the desorbed forms for the *syn*-[**PdPt**] and *syn*-[**PtPt**] salts are close to those in solution. Considering the short intermolecular Pt⋯Pt distances for the CH_3CN-included forms in the *syn*-[**PdPt**] and *syn*-[**PtPt**] salts (ca. 3.37 Å), the red-shifts for the vapour-included forms were attributable to the lowering of the MMLCT transition energy due to the *inter*molecular Pt⋯Pt interactions between the two dinuclear motifs. The conceptual MO energy diagram is
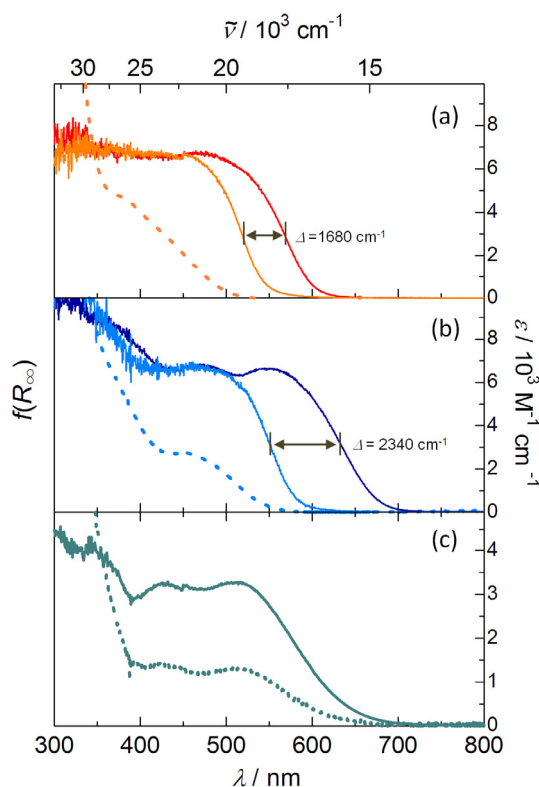

Fig. 5 Diffuse reflectance spectra for hexaflurophosphate of (a) *syn*-[**PdPt**], (b) *syn*-[**PtPt**], and (c) *syn*-[**AuPt**]: orange and light blue solid lines are for the desorbed forms, B and E in Fig. 4, and red blue, and blue solid lines are those under exposure to CH_3CN vapour, respectively. The dotted lines exhibit the solution spectra in CH_3CN with the scale on the right.

shown in Scheme 3. It is also interesting to note that the spectral change for the *syn*-[**PdPt**] salt occurs in a high-energy region compared with that of the *syn*-[**PtPt**] salt. This indicates that the chromic region is controlled by the *intra*molecular metal-metal interaction. Additionally, taking into account that the vapochromic shift is larger for *syn*-[**PtPt**] ($\Delta = 2,340$ cm^{-1}) than for *syn*-[**PdPt**] ($\Delta = 1,680$ cm^{-1}), where Δ denotes the energy difference in wavenumbers of the vapour-included and desorbed spectra at the positions with half intensity, the intramolecular metal-metal interaction could affect the intermolecular metal-metal interaction. The influence of the outer metal site on the intermolecular Pt⋯Pt interaction was also suggested by the series of corresponding *syn*-[**CuPt**] systems bearing different axial ligands on the Cu(II) site.[20]
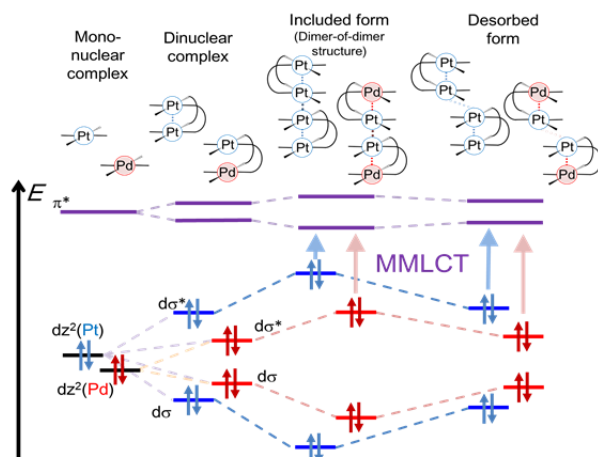
Scheme 3 Conceptual MO energy diagram for *syn*-[**PdPt**] and *syn*-[**PtPt**].

Structural transformation induced by vapour. To clarify the structural factors of the colour change induced by the absorption/desorption of vapour molecules, we next carried out single-crystal diffraction measurements at various temperatures. Figure 6 shows the changes in the lattice constants of the dark-red form of *syn*-[**PtPt**] with increasing temperature from −180°C under nitrogen gas flow. A drastic change in the lattice parameters occurred at 0°C while retaining the same orthorhombic crystal system. Concomitantly, a clear colour change in the crystal was also observed from dark-red to light-red (Fig. 6, inset photos). By using a thus-obtained single crystal of the light-red form, we succeeded in determining the crystal structure of the light-red form. Though the quality of the diffraction data for the light-red form was not very high, it was sufficient to determine the arrangement of the light-red form of *syn*-[**PtPt**]. As a result, a significantly shifted arrangement of the dimer-of-dimer structure was elucidated (Fig. 7 and Fig. S6). For the light-red form, the intermolecular Pt⋯Pt contact that has been observed in the crystal of the dark-red form is completely broken and replaces by the π-π stacking of the bpy ligands. Although the dimer structure of the complex unit was essentially the same for both forms, the intramolecular Pt⋯Pt distance (2.876(2) Å) is slightly shorter compared to that of the dark-red form (2.9168(3) Å), which could be due to the breaking of the intermolecular Pt⋯Pt interaction (Pt⋯Pt (intermolecular) = 5.508(2) Å). The
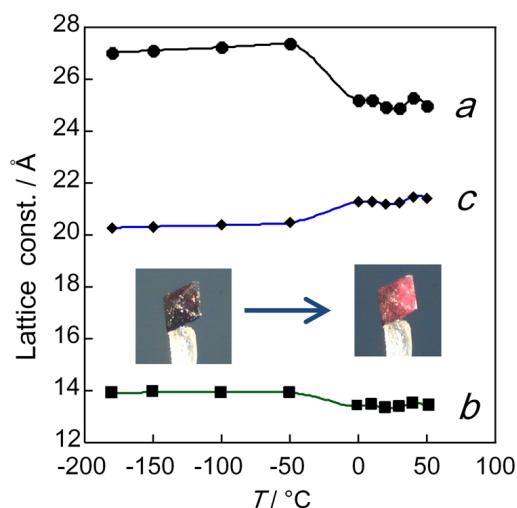
Fig. 6 Plots of the lattice constants (*a*, *b*, and *c*) of *syn*-[**PtPt**](PF₆)₂-1.5 CH₃CN at various temperatures upon heating from −180 to 50°C. Inset: Photographs of the sample crystal before and after a series of measurements.
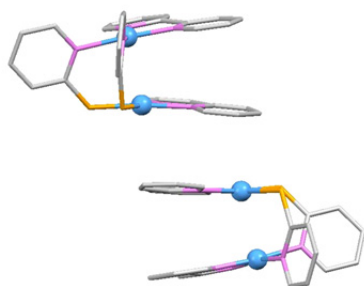

Fig. 7 Shifted dimer-of-dimer structure for the light-red form of *syn*-[**PtPt**]. The nearest Pt···Pt distance between the two dinuclear units is 5.508(2) Å.

transformation of the dimer-of-dimer structure is induced by the release of CH₃CN molecules included in the dark-red form, followed by sliding so as to fill the void space.

5   The reversible structural transformations driving the vapochromic behaviours of *syn*-[**PtPt**] and *syn*-[**PdPt**] were confirmed by powder X-ray diffraction (PXRD). As shown in Fig. 8, the PXRD pattern of *syn*-[**PtPt**] changed between the vapour-included and desorbed forms repeatedly, corresponding to the

10 changes in the diffuse reflectance spectra upon repeated heating at 50°C and CH₃CN vapour exposure. Essentially the same changes of the PXRD pattern as those for *syn*-[**PtPt**] were observed for the isomorphous *syn*-[**PdPt**] (Fig. S7). These results clearly indicate that the vapochromism of *syn*-[**PtPt**] and *syn*-

15 [**PdPt**] occurs essentially by the same mechanism, which is based on the structural transformation of the intermolecular Pt···Pt interaction between the dinuclear units, i.e. an ON-OFF switch. The fact that *syn*-[**AuPt**], which lacked the dimer-of-dimer structure, exhibited no vapochromic behaviour also supports this

20 mechanism.

In addition, we investigated the responses of *syn*-[**PdPt**] and *syn*-[**PtPt**] to other organic vapours. As shown in Fig. 9, similar
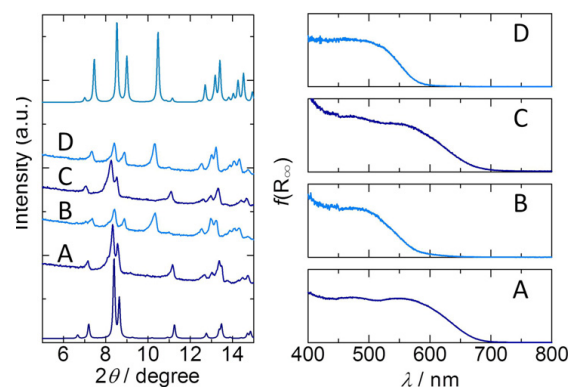

Fig. 8 Reversible vapochromic response of *syn*-[**PtPt**]. Left: The PXRD pattern changes in the repeated cycles of CH₃CN vapour exposure (A and C) and after heating at 80°C (B and D). Top and bottom patterns are the calculated ones on the basis of the single-crystal structures of the light-red and dark-red forms, respectively. Right: The diffuse reflectance spectra of the samples corresponding to the PXRD data.

spectral changes were observed on exposure to vapours of small organic molecules such as methanol, acetone, tetrahydrofuran

25 (THF), and formaldehyde, while no changes occurred for vapours with relatively lower polarity, such as chloroform, *n*-hexane, and carbon tetrachloride. The samples which underwent colour changes by the former vapours exhibited the PXRD patterns of the vapour-included forms (Fig. S8). These results suggest that

30 the structural transformations due to vapour sorption of these complexes generated essentially the same dimer-of-dimer structure with short Pt···Pt contacts as that found for the CH₃CN vapour. On the other hand, there are no changes in the PXRD patterns of the desorbed forms in the cases of hexane and carbon

35 tetrachloride vapours. It is interesting to note that some structural transformation occurred in the presence of chloroform vapour, resulting in another structure with no Pt···Pt close contact
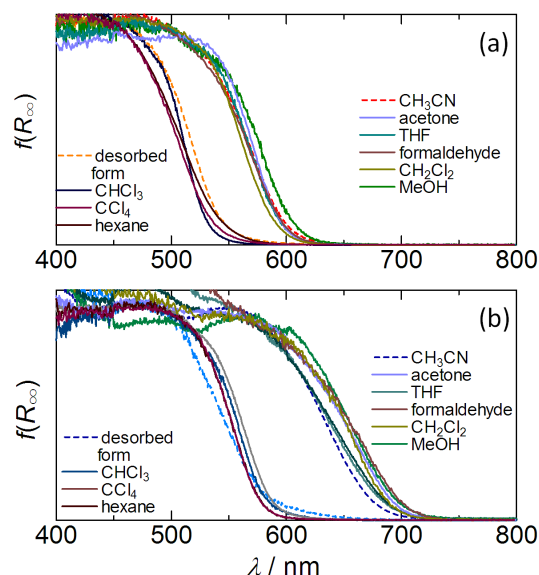

Fig. 9 Diffuse reflectance spectra for (a) *syn*-[**PdPt**] and (b) *syn*-[**PtPt**] under various solvent vapours.

between the dinuclear motifs. These results suggest that the vapochromic response of these complexes depends on whether the dimer-of-dimer structure with the Pt⋯Pt close contact can be formed by taking up the vapour. Such vapochromic dinuclear systems are quite unique; most vapochromic systems consist of mononuclear complexes assembled by metallophilic interactions. Only a few examples of dinuclear complexes whose chromic origins are π-π interactions and halogens have been reported.[2m-o]

Mechanochromic behaviour. In the course of the investigation of the vapochromic response, we also found that the complexes exhibited mechanochromic behaviour. The desorbed forms of *syn*-[**PtPt**] and *syn*-[**PdPt**] are air-stable at room temperature. However, when they were ground in agate mortars, distinct colour changes occurred even in the absence of vapour, from orange to red for *syn*-[**PdPt**], and from light-red to dark-red for *syn*-[**PtPt**] (Figs. 4C and 4F, respectively). The diffuse reflectance spectra of the ground samples exhibited large red shifts compared with those of the desorbed forms, extending to slightly longer wavelengths than those of the corresponding vapour-included forms (Fig. S9). The samples after grinding did not exhibit any diffraction peaks (Fig. S10), indicating that the desorbed crystalline forms of *syn*-[**PtPt**] and *syn*-[**PdPt**] were transformed to amorphous forms by grinding. The amorphous states were also obtained by grinding the vapour-included forms. Such mechanochromic behaviours based on a crystalline-to-amorphous transformation by grinding were reported recently.[21] For example, Ito et al.[21a] found that the Au(I) complex, $[(C_6F_5Au)_2(\mu$-1,4-diisocyanobenzene)] exhibited mechanochromic luminescence due to the formation of a Au⋯Au interaction by grinding, and Chen et al.[21b] reported the case of platinum(II) complexes containing 5-trimethylsilylethynyl-2,2′-bipyridine and phenylacetylide. We also reported a coordination polymer with the formula $[Mg(H_2O)_5][Pt(CN)_2(4,4′$-dcbpy)] (4,4′-dcbpy = 4,4′-dicarboxy-2,2′-bipyridine) which exhibited multichromic behaviour by grinding and vapour exposure.[2i] These results suggest that metal-metal interactions often occur in the amorphous state by grinding, forming short, local metal-metal contacts. Interestingly, the vapour-included forms were reconstructed on exposure to CH_3CN vapour, as shown by the recovered PXRD patterns and absorption spectra for both *syn*-[**PdPt**] and *syn*-[**PtPt**] systems (Fig. S10). Therefore, taking into account the relatively stable dinuclear framework of *syn*-[**MPt**] in the solid, it would be reasonable that the intermolecular Pt⋯Pt interaction between the dinuclear motifs could also occur mechanically by the collapse of the crystal structure. It is noteworthy that structural reconstruction was not observed by heating to 50°C, at which the structural transformations occurred from the included to the desorbed forms. This indicates that vapour molecules play an essential role to control the structural construction and transformation.

Conclusion

In addition to homometallic platinum dinuclear complexes bridged by pyridinethiolate ligands, we synthesized a series of heterodinuclear complexes by stepwise complexation. The mechanism of the vapochromism characteristic of *syn*-[**PdPt**](PF$_6$)$_2$ and *syn*-[**PtPt**](PF$_6$)$_2$ was clarified on the basis of X-ray diffraction studies, including a single-crystal to single-crystal transformation and powder diffraction. The vapochromic behaviour arises by the formation and breaking of the intermolecular Pt⋯Pt interaction induced by the absorption and desorption of the vapour molecules. It is noteworthy that the energy region of the colour change can be controlled by the introduction of different metal ions, from red to orange for *syn*-[**PdPt**] and from dark-red to light-red for *syn*-[**PtPt**]. The vapochromic mechanism was also supported by the facts that neither *syn*-[**AuPt**] having a discrete dimer structure nor *anti*-[**PdPt**] with only loose stacking exhibited such vapochromic responses. Furthermore, these complexes were found to exhibit mechanochromic behaviour, through the crystal-to-amorphous transformation, by grinding. The overall chromic behaviour of these dinuclear complexes is summarized in Scheme 4.

The dinuclear complexes constructed using a planar ligand (bpy) and two bridging ligands containing two different coordinating atoms (pyt) constituted a good molecular motif through which to assemble metal ions and control both *intra*- and *inter*molecular metal-metal interactions. Taking advantage of the regioselective introduction of the heterometal ions into the same molecular motif, further investigations of *syn*-[**MPt**] complexes including 3d metal ions are now in progress.
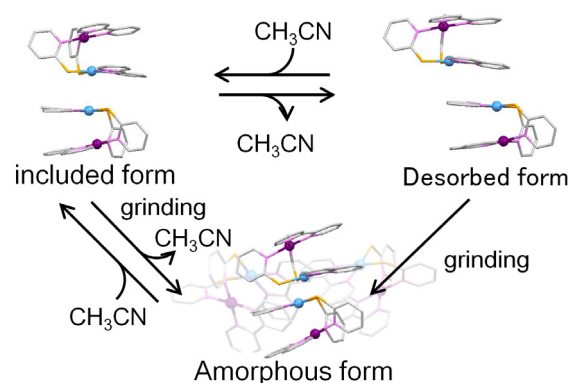
Scheme 4 Structural transformations of the dimer-of-dimer motif of *syn*-[**MPt**] (M = Pd^{2+} and Pt^{2+}) induced by vapour and grinding.

Notes and references

Department of Chemistry, Faculty of Science, Hokkaido University, North-10 West-8, Kita-ku, Sapporo, Hokkaido 060-0810, Japan. Fax: +81-11-7063447; Tel: +81-11-7063817; E-mail: mkato@sci.hokudai.ac.jp

† Electronic Supplementary Information (ESI) available: ^{1}H NMR spectral changes showing the isomerisation from *syn*-[**PdPt**] to *anti*-[**PdPt**]; FAB-MS spectrum of *anti*-[**PdPt**]; vapour-adsorbed isotherm and thermogravimetric curves of *syn*-[**PdPt**](PF$_6$)$_2$; the crystallographic data

and the structure of the light-red form of *syn*-[**PtPt**](PF$_6$)$_2$; PXRD patterns for *syn*-[**PdPt**] and *syn*-[**PtPt**] under various vapours; diffuse reflectance spectra and PXRD results for the ground samples of *syn*-[**PdPt**] and *syn*-[**PtPt**]. See DOI: 10.1039/b000000x/

5   1   (*a*) X. Zhang, B. Ki, Z.-H. Chen, and Z.-N. Chen, *J. Mater. Chem.*, 2012, **22**, 11427; (*b*) M. A. Moansour, W. B. Connick, R. J. Lachicotte, H. J. Grysling, and R. Eisenberg, *J. Am. Chem. Soc.* 1998, **120**, 1329; (*c*) E. Cariati, X. Bu, and P. C. Ford, *Chem. Mater.*, 2000, **12**, 3385; (*d*) L. G. Beauvais, M. P. Shores, and J. R. Long, *J. Am, Chem. Soc.*, 2000, **122**, 2763; (*e*) E. J. Fernandez, J. M. Lopez-de-Luzuriaga, M. Monge, M. E. Olomos, R. C. Puelles, A. Laguna, A. A. Mohamed, and J. P. Fackler, *Inorg. Chem.*, 2008, **47**, 8069; (*f*) M. Albrecht, M. Lutz, A. L. Spek, and G. Koten, *Nature*, 2000, **406**, 970; (*g*) A. Kobayashi, M. Dosen, M. Chang, K. Nakajima, S. Noro, and M. Kato, *J. Am. Chem. Soc.*, 2010, **132**, 15286; (*h*) Z. Fri, N. Koche, C. J. Mohrschladt, H. Ihmels, and D. Stalke, *Angew. Chem. Int. Ed.*, 2003, **42**, 783; (*i*) T. Hinoue, M. Miyata, I. Hisaki, and N. Tohnai, *Angew. Chem. Int. Ed.*, 2012, **51**, 155.

  2   (*a*) M. Kato, *Bull. Chem. Soc. Jpn.*, 2007, **8**, 287; (*b*) S. M. Drew, D. 20 E. Janzen, C. E. Buss, D. I. MacEwan, K. M. Dublin, and K. R. Mann, *J. Am. Chem. Soc.*, 2001, **123**, 8418; (*c*) T. J. Wadas, Q.-M. Wang, Y. J. Kim, C. Flaschenriem, T. N. Blaton, and R. Eisenberg, *J. Am. Chem. Soc.*, 2004, **126**, 16841; (*d*) L. J. Grove, J. M. Rennekamp, H. Jude, and W. B. Connick, *J. Am. Chem. Soc.*, 2004, **126**, 1594; (*e*) M. 25 L. Muro, C. A. Daws, and F. N. Castellano, *Chem. Commun.*, **2008**, 6134; (*f*) A. Kobayashi, Y. Fukuzawa, H.-C. Chang, and M. Kato, *Inorg. Chem.*, 2012, **51**, 7508; (*g*) Z. M. Hudson, C. Sun, K. J. Harris, B. E. G. Lucier, R. W. Schurko, and S. Wang, *Inorg. Chem.*, 2011, **50**, 3447; (*h*) J. Ni, Y.-H. Wu, X. Zhang, B. Li, L.-Y. Zhang, and Z.- 30 N. Chen, *Inorg. Chem.*, 2009, **48**, 10202; (*i*) A. Kobayashi, H. Hara, T. Yonemura, H.-C. Chang, and M. Kato, *Dalton. Trans.*, 2012, **41**, 1878; (*j*) A. Kobayashi, H. Hara, S. Noro, and M. Kato, *Dalton. Trans.*, 2010, **39**, 3400; (*k*) H. Hara, A. Kobayashi, S. Noro, H.-C. Chang, and M. Kato, *Dalton. Trans.*, 2011, **40**, 8012; (*l*) P. Du, J. 35 Schneider, W. W. Brennessel, and R. Eisenberg, *Inorg. Chem.*, 2008, **47**, 69; (*m*) I. Mathew, Y. Li, Z. Li, and W. Sun, *Dalton. Trans.*, 2010, **39**, 11201; (*n*) S. C. F. Kui, S. S.-Y.Chui, C.-M Che, and N. Zhu, *J. Am. Chem. Soc.*, 2006, **128**, 8297; (*o*) H. Mastuzaki, H. Kishida, H. Okamoto, K. Takizawa, S. Matsunaga, S. Takaishi, H. Miyasaka, K. 40 Sugiura and M. Yamashita, *Angew. Chem., Int. Ed*., 2005, **44**, 3240.

  3   M. Kato, A. Omura, A. Toshikawa, S. Kishi, and Y. Sugimoto, *Angew. Chem. Int. Ed.,* 2002, **41**, 3183.

  4   (*a*) J. K. Barton, H. N. Rabinowitz, D. J. Szalda, and S. J. Lippard, *J. Am. Chem. Soc.*, 1977, **99**, 2827; (*b*) J. P. Laurent, P. Lepage, and F. 45 Dahan, *J. Am. Chem. Soc.*, 1982, **104**, 7335; (*c*) L. S. Hollis and S. J. Lippard, *J. Am, Chem. Soc.*, 1981, **103**, 1230; (*d*) K. Matsumoto and M. Ochiai, *Coord. Chem. Rev.*, 2002, **231**, 229; (*e*) K. Sakai, K. Takeshita, Y. Tanaka, T. Ue, M. Yanagisawa, M. Kosaka, T. Tsubomura, M. Ato, and T. Nakano, *J. Am. Chem. Soc.*, 1998, **120**, 50 11353.

  5   T. J. Egan, K. R. Koch, P. L. Swan, C. Clarkson, D. A. V. Schalkwyk, and P. J. Smith, *J. Med. Chem.,* 2004, **47**, 2926.

  6   M. Noskowska, E. Śliwińska, and W. Duczmal, *Transition Met. Chem.,* 2003, **28**, 756.

55   7   J. K. Bjernemose, P. R. Raithby, and H. Toftlund, *Acta Cryst.*, 2004, **E60**, m1719.

  8   B.-C. Tzeng, W.-F Fu, C.-M. Che, H.-Y. Chao, K.-K. Cheung, and S.-M. Peng, *J. Chem. Soc., Dalton Trans.,* 1999, 1017.

  9   *CrystalClear*, Molecular Structure Corporation, Orem, UT, 2001.

60 10 *SIR92*: A. Altomare, G. Cascarano, C. Giacovazzo, A. Guagliardi, M. Burla, G. Polidori, and M. Camalli, *J. Appl. Cryst.,* 1994, **27**, 435.

11 *DIRDIF99*, P. T. Beurskens, G. Admiraal, G. Beurskens, W. P. Bosman, R. de Gelder, R. Israel, and J. M. M. Smits (1999).

12 *CrystalStructure 3.8*, Crystal Structure Analysis Package, Rigaku and 65 Rigaku/MSC (2000-2006), 9009 New Trails Dr., The Woodlands, TX 77381 USA.

13 *SHELX97*, G. M. Sheldrick, *Acta Crystallogr., Sect. A*, 2008, **64**, 112.

14 L. Yin, P. J. S. Miguel, W. Hiller, and B. Lippert, *Inorg. Chem.*, 2012, **51**, 6784.

70 15 K. Matsumoto, and H. Urata, *Chem. Lett.,* **1993**, 2061.

16 (*a*) R. Hayoun, D. K. Zhong, A. L. Rheingold, and L. H. Doerrer, *Inorg. Chem.* 2006, **45**, 6120; (*b*) L. H. Doerrer, *Dalton Trans.*, 2010, **39**, 3543; (*c*) M. Stender, R. L. White-Morris, M. M. Olmstead, and A. L. Balch, *Inorg. Chem.,* 2003, **42**, 4504.

75 17 C.-W. Chan, W.-T. Wong, and C.-M. Che, *Inorg. Chem.,* 1994, **33**, 1266.

18 V. W.-W. Yam, K. M.-C. Wong, L.-L. Hung, and N. Zhu, *Angew. Chem. Int. Ed.,* 2005, **44**, 3107.

19 J. D. Crowley, and B. Bosnich, *Inorg. Chem.,* 2005, **44**, 2989.

80 20 T. Ohba, A. Kobayashi, H.-C. Chang, and M. Kato, to be submitted.

21 (*a*) Y. Sagara, and T. Kato, *Nature Chem.*, 2009, **1**, 605; (*b*) Y.-A. Lee, and R. Eisenberg, *J. Am. Chem. Soc.*, 2003, **125**, 7778; (*c*) B. R. Crenshaw, and C. Weder, *Chem. Mater.*, 2003, **15**, 4717; (*d*) Y. Sagara, T. Mutai, I. Yoshikawa, and K. Araki, *J. Am. Chem. Soc.*, 85 2007, **129**, 1520; (*e*) Y. Sagara, T. Kato, *Angew. Chem. Int. Ed.*, 2008, **47**, 5175; (*f*) G. Zhang, J. Lu, M. Sabat, and C. L. Fraser, *J. Am. Chem. Soc.*, 2010, **132**, 2160; (*g*) M. Osawa, I. Kawata, S. Igawa, M. Hoshino, T. Fukunaga, and D. Hashizume, *Chem. Eur. J.*, 2010, **16**, 12114; (*h*) A. Abedi, N. Safari, V. Amani, and H. R. Khavasi, *Dalton* 90 *Trans.*, 2011, **40**, 6877; (*i*) G. Zhang, J. Lu, and C. L. Fraser, *Inorg. Chem.*, 2010, **49**, 10747; (*j*) Y. Ren, W. H. Kan, V. Thangdfurai, and T. Baumgartner, *Angew. Chem. Int. Ed.*, 2012, **51**, 3964.

21 (*a*) H. Ito, T. Saito, N. Oshima, N. Kitamura, S. Ishizaka, Y. Hinatsu, M. Wakeshima, M. Kato, K. Tsuge, and M. Sawamura, *J. Am. Chem.* 95 *Soc.*, **2008**, 130, 10044; (*b*) J. Ni, X. Zhang, N. Qiu, Y.-H. Wu, L.-Y. Zhang, J. Zhang, and Z.-N. Chen, *Inorg. Chem.*, 2011, **50**, 9090; (*c*) Y. Sagara, T. Mutai, I. Yoshikawa, and K. Araki, *J. Am. Chem. Soc.*, 2007, **129**, 1520; (*d*) M. Osawa, I. Kawata, S. Igawa, M. Hoshino, T. Fukunaga, and D. Hashizume, *Chem. Eur. J.*, 2010, **16**, 12114.

100